Supplementary Material

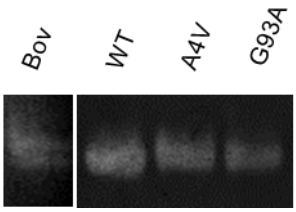

Supplementary Fig. 1. Activity Gel. Superoxide dismutase activity was detected for each of the highly purified human SOD1 proteins used in this study. Activity bands developed on native gels loaded with 500 ng of WT, A4V, and G93A SOD1s and bovine SOD1 (Bov, as positive control).

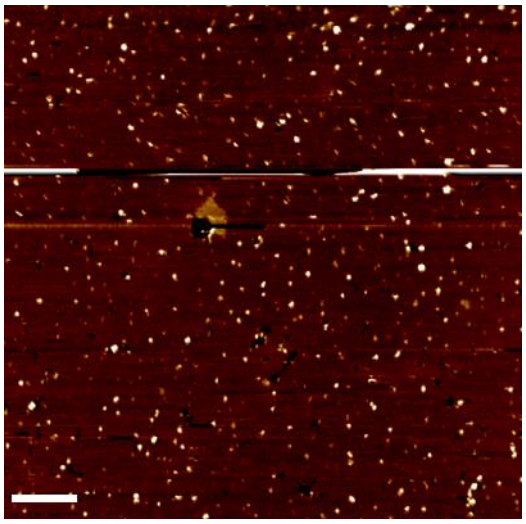

Supplementary Fig. 2. Lower resolution AFM scan in HBS buffer confirms G93ASOD1 binds the curved lipid bilayer of DOPG liposomes which following binding are fused to form the planar bilayer shown. Membrane-bound G93ASOD1 particles are visualized dotting the DOPG surface. Full scale z-axis, 10 nm. Bar, 250 nm

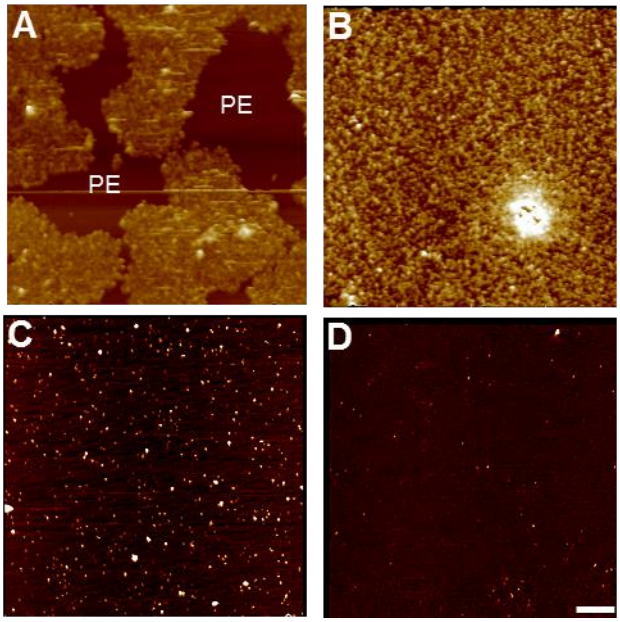

Supplementary Fig. 3. HRF-AFM shows A4VSOD1 binds PG bilayers similar to that of G93ASOD1 while WTSOD1 binding to PG is low. 100 nM A4VSOD1 on (A) mixed bilayer of 3:1 DOPG:DOPE (B) DOPG bilayer and (C) 50 nM A4VSOD1 on DOPG and (D) low binding of 100 nM WTSOD1 on DOPG bilayer, in HBS for all. Full scale z-axis, 5 nm. Bar, 250 nm for all.

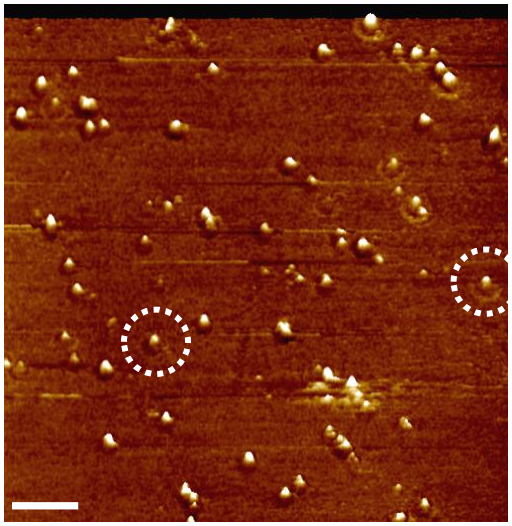

Supplementary Fig. 4. HRF-AFM reveals binding of (dashed circles) ~25 nm supramolecular P188 to DOTAP lipid bilayer. A supported bilayer of 1,2 dioleoyl-3- tri-methyl ammonium propane (DOTAP, Avanti Polar Lipids, Alabaster, AL) was imaged by HRF-AFM before and after incubation of 50 µM P188 in HBS atop the bilayer. Interestingly, although the presence of P188 molecules loosely interacting near the bilayer surface could be detected, consistent with previous reports (Banquy et al., 2015), HRF-AFM could not produce clear images of P188 bound to PG or to any of our panel of naturally-occurring model membranes (i.e., PG, PE, PS, PE, PA). Full scale z-axis, 7 nm. Bar, 250 nm.

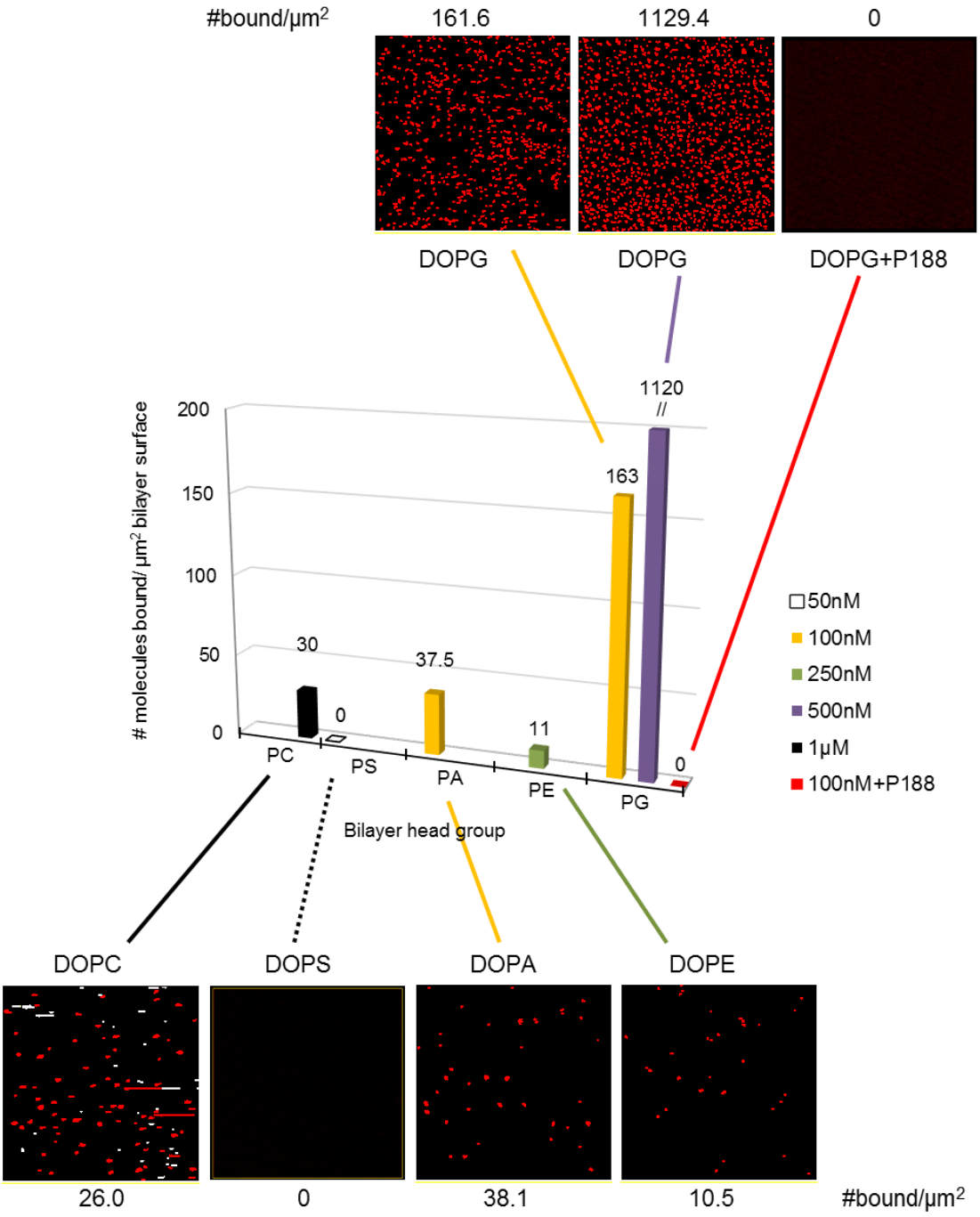

Supplementary Fig. 5. AFM-based quantitation of G93ASOD1 binding densities on five different supported lipid bilayer targets. Counts of the densities (#bound/μm^2) of membrane-bound G93ASOD1 protein (red dots) using varying concentrations of G93ASOD1, reveals the strong preference of G93ASOD1 for DOPG.

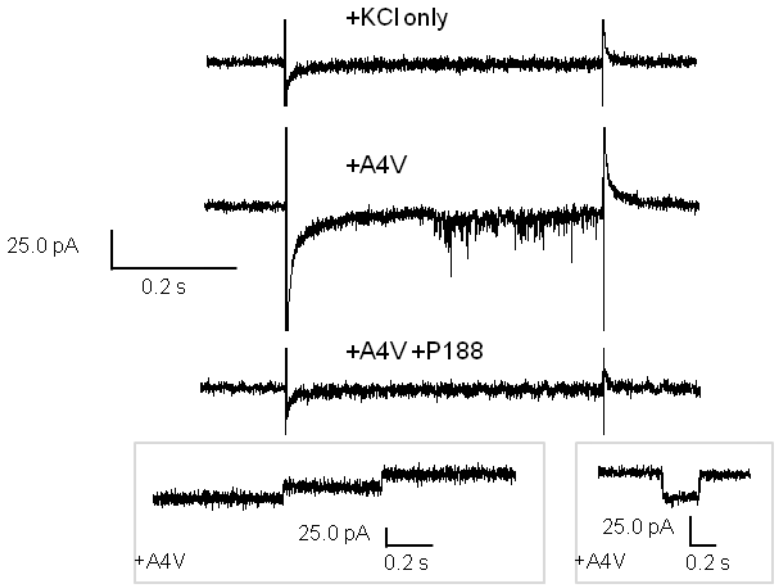

Supplementary Fig. 6. SB-EP shows P188 suppresses A4VSOD1 membrane toxicity. Trace recordings A4VSOD1 against PG:PE membrane (3:1, w/w) showing channel-like activity in 150 mM KCl (middle trace and both boxed insets). The bottom of three traces shows this activity is blocked in the presence of P188. The “toxic channel” activity of A4VSOD1 was observed in 100% of trials, as frequently as the positive control, alpha-hemolysin.

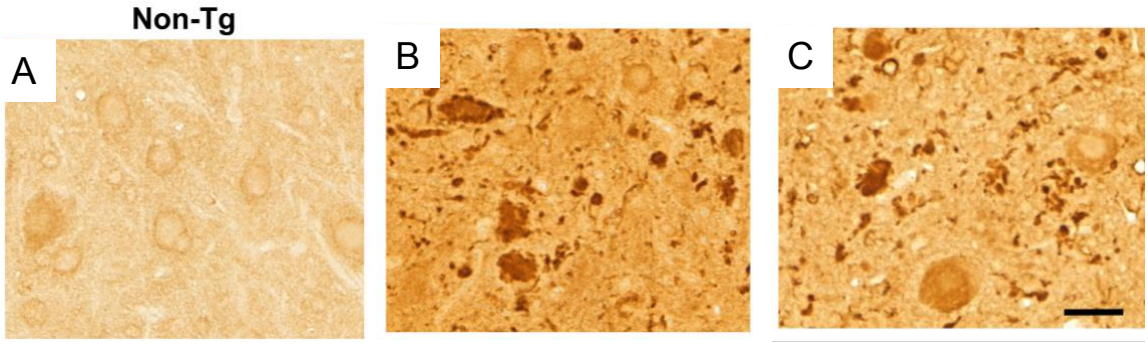

Supplementary Fig. 7. Four similarly aged (A) non-transgenic, (B) aCSF-treated, and (C) P188-treated endstage G93ASOD1 mice were sacrificed and lumbar spinal cords stained for SOD1 aggregation. Inspection of at least 20 spinal cord sections found no differences in SOD1 aggregate size and number between aCSF-treated mice and P188-treated mice (B *vs* C). We speculate this result is an indication of the greater toxicity of small soluble SOD1 oligomers, the precursors to aggregation (too small to resolve by light microscopy), compared to the lighter burden of large insoluble cytoplasmic SOD1 aggregates. Bar, 50 µm.

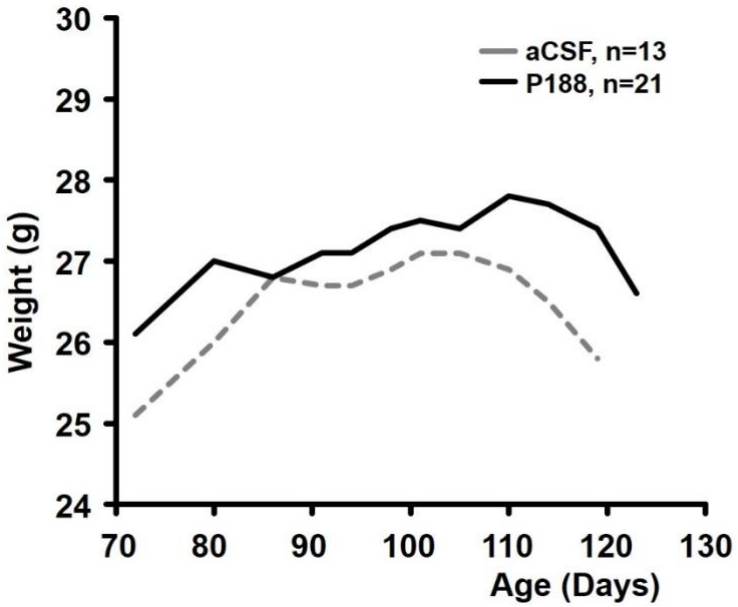

Supplementary Fig. 8. Body weight showed no statistical differences at any time point between the two mouse groups (P>0.05). Mean body weight was presented from 72 days of age for both groups until the time that the first mouse within either group had reached end-stage, i.e.,119 days of age for aCSF-treated mice (n=13) and 123 days of age for P188-treated mice (n=21).

References

Banquy, X., Lee, D. W., Kristiansen, K., Gebbie, M. A., & Israelachvili, J. N. [2015]. Interaction forces between supported lipid bilayers in the presence of PEGylated polymers. *Biomacromolecules*, *17*(1), 88–97